Microstructure of bentonites: characterisation and evolution under mechanical and environmental loads

Anne-Catherine Dieudonné

Delft University of Technology, the Netherlands

1 Introduction

The role of engineered barriers in geological disposal of radioactive waste is to form a tight contact with the host rock, and thereby limit the release of radionuclides to the biosphere. The low permeability and important swelling capacity of bentonites are therefore essential properties. In order to characterize the swelling capacity of compacted bentonites, two macroscopic physical quantities can be measured: the swelling potential and the swelling pressure. These quantities are determined after saturation of a bentonite sample under different confining conditions. The swelling potential $\Delta H/H_i$ corresponds to the ratio between the change in sample height ΔH upon saturation under oedometer conditions, and its initial height H_i. On the contrary, the swelling pressure S_P is defined as the pressure required to prevent volume changes upon wetting. Figure 1 presents the evolution of the swelling pressure of five reference bentonites with dry density. While important differences are observed between the different bentonites, they all show an increase of their swelling pressure with dry density. Furthermore, the swelling pressures reached upon saturation (typically of the order of few MPa to around 15 MPa for dry densities ranging between 1.5 and 1.7 Mg/m^3) are significantly higher than for non-swelling clays (few hundreds kPa).

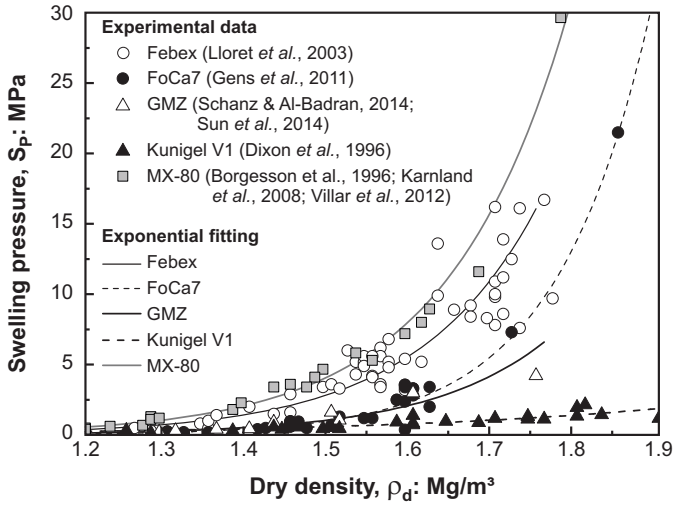

Figure 1: Evolution of the swelling pressure of five reference bentonites with dry density.

While the swelling capacity of compacted bentonite is firstly observed at the macroscopic scale, this property essentially results from physicochemical phenomena taking place at a microscopic scale. Therefore, a good comprehension of the material microstructure is of paramount importance for a better understanding of the hydromechanical behaviour of compacted bentonites and for the development of physically-based constitutive models.

These lecture notes are organized as follows. The mineralogical composition of bentonites is first presented. The structure and coupled processes taking place in compacted bentonites are then described

starting from the smallest scale of interest, namely the scale of the clay minerals. Accordingly, the structure and physicochemical properties of clay minerals are presented. Attention is then focused on the hydration and swelling mechanisms in smectites, the main constituents of bentonites. Increasing the scale of observation, the structure of compacted bentonites is addressed. The water storage and hydration mechanisms are analysed. The different factors, both mechanical and environmental, affecting the material structure are presented. Finally, modelling challenges and prospects are addressed.

2 Definition and mineralogical composition of bentonites

The name bentonite dates back to the late 19th century when Knight [1898] used the term to describe highly plastic and swelling clays from the Cretaceous Fort Benton group in Wyoming, USA. The first definitions of bentonite [Hewitt, 1917; Wherry, 1917; Ross & Shannon, 1926] suggested a genetic origin of the material, generally from the alteration of tuff or volcanic ash. Nowadays, the term bentonite has lost its mineralogical definition and refers to any smectite-rich material regardless of its geological origin [Grim, 1968]. More specifically, in the context of nuclear waste disposal, bentonite primarily consists of montmorillonite, a clay mineral of the smectite group which exhibits significant swelling upon hydration [Apted, 1995].

Table 1 presents the mineralogical composition of five reference bentonites which are studied as potential barriers for the isolation of high-level and intermediate-level radioactive waste. Besides montmorillonite, these bentonites contain variable quantities of other clay minerals (generally kaolinite and illite, which are non-swelling clay minerals), quartz[1], feldspars, plagioclase, gypsum, pyrite and calcite. They can also hold small amounts of organic matter (usually less than 0.5%). Although present in limited quantities, some of these accessory minerals may influence the properties of bentonites, especially their chemical reactivity [Sellin & Leupin, 2013].

Bentonite	Origin	Phyllosicilicate	SiO_2	K-feldspar	Plagioclase
Febex[a]	Spain	92% interstratified montmorillonite–illite (10–15% illite)	2%	traces	2%
FoCa7[b]	France	80–85% interstratified smectite–kaolinite (50% Ca-beidellite, 50% kaolinite) 4–6% kaolinite	1.4–6%		
GMZ[c]	China	75.4% montmorillonite 0.8% kaolinite	20%	4.3%	
Kunigel V1[d]	Japan	46–49% montmorillonite	29–38%	2.7–5.5%	4%
MX-80[e]	USA	75–90% montmorillonite	2.8–15.2%	2–8%	9.2%

[a] Fernandez [2004], Lloret & Villar [2007]
[b] Proust *et al.* [1990], Bruno [1993], Lajudie *et al.* [1994]
[c] Wen [2006]
[d] JNC [2000], Nakashima [2004]
[e] Lajudie *et al.* [1994], Madsen [1998], Montes-H [2002]

Table 1: Mineralogical composition (main minerals) of five reference bentonites.

[1] In Table 1, the content in SiO_2 corresponds to the total content in quartz, cristobalite and tridymite.

3 Structure of clay minerals

3.1 Structure and mineralogy

Clay minerals belong to the phyllosilicate group. The term phyllosilicate derives from the Greek *phyllon*, leaf, emphasizing the layered structure of clay minerals. This structure is based on the combination of two basic crystal structural units, namely the tetrahedral sheet and the octahedral sheet.

The tetrahedral sheet is also called silica sheet. As shown in Figure 2(a), it is made up of silica tetrahedra $(SiO_4)^{4-}$, which are linked together by sharing three of their four oxygen ions. All tetrahedra of the silica sheet are oriented in the same direction and define hexagonal cavities. Similarly, Figure 2(b) shows the structure of the octahedral sheet, also termed alumina sheet. The octahedral sheet is composed of aluminium or magnesium octahedra in which the cation bonds with six oxygen atoms or hydroxyl groups. Octahedra are all laid on a triangular face and linked together by sharing their six oxygens or hydroxyls.

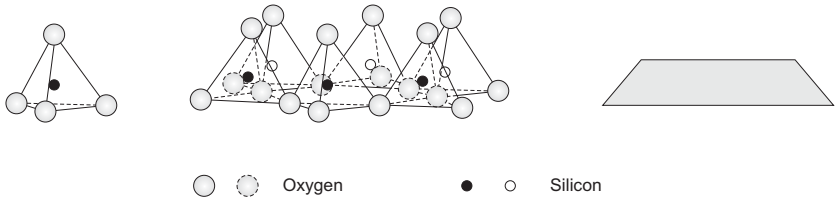

(a) Silica tetrahedron, tetrahedral sheet and schematic representation of the tetrahedral sheet.

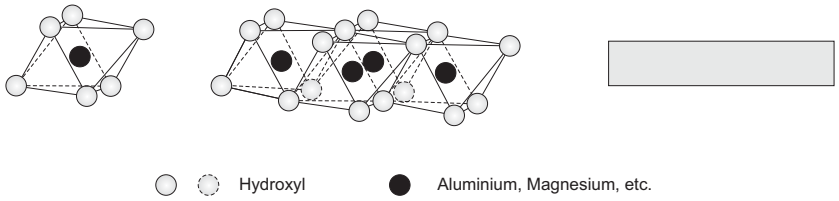

(b) Aluminium or magnesium octahedron, octahedral sheet and schematic representation of the octahedral sheet.

Figure 2: Basic crystal structural units of phyllosilicates [Mitchell & Soga, 2005].

Tetrahedral and octahedral sheets bond together to form layers. Two types of layers are defined, namely the TO layer and the TOT layer. The TO layer, also called 1:1 layer, is made up of one tetrahedral sheet and one octahedral sheet, and has a thickness of 7.2 Å. On the other hand, the TOT layer, or 2:1 layer, consists of an octahedral sheet sandwiched between two tetrahedral sheets. Its thickness in the absence of any polar molecule is 9.6 Å. In both cases, strong primary bonds exist between the sheets of a same layer [Stçepkowska, 1990].

Conversely, the bonds between two successive layers are generally weaker. The type of layers and the nature of the interlayer determine the properties of the different clay minerals and, in particular, their behaviour in presence of water. On this basis, clay minerals are classified into different groups, as depicted in Figure 3. The main clay minerals composing bentonites, namely smectite, kaolinite and illite, are to be found in this classification.

The structure of kaolinite is based on the TO layer, whereas the structures of smectite and illite are built on the TOT layer. In kaolinite, hydroxyl groups and oxygen ions of two consecutive layers are bonded through hydrogen bonds which maintain the interlayer closed and prevent swelling. Only the external surfaces can adsorb water, allowing limited swelling. In smectites, water molecules and ions are able to penetrate the interlayer space, causing the expansion of the mineral upon wetting. Conversely, the interlayer space of illite is occupied by potassium ions whose molecular size is close to the one of the hexagonal cavities of the tetrahedral sheet, and which therefore strongly lock the layers together through ionic bonds, thereby preventing swelling. When layers of different types are stacked together, the mineral is referred to as a mixed-layer or interstratified mineral, and its behaviour depends on the nature of the different layers and interlayers.

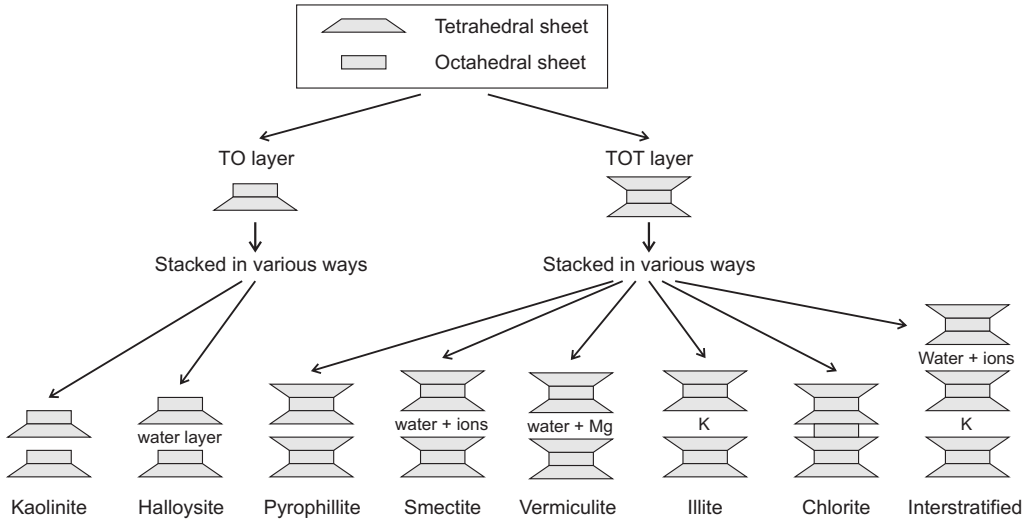

Figure 3: Classification of clay minerals [Mitchell & Soga, 2005].

Finally, clay layers stack together to form particles. Depending on the nature of the interlayer and the water content, the number of layers in a particle may vary from a few to several hundreds [Saiyouri *et al.*, 2004]. The behaviour of the different clay minerals in presence of water is further discussed in the next two sections, with a special attention given to smectites.

3.2 Physicochemical properties

A fundamental characteristic of clay minerals is their electronegativity. The surface of phyllosilicates is indeed not electrically neutral and surface charges exist (Table 2). These charges have two different origins:

- **Isomorphous substitutions**, which refer the replacements of ions in the tetrahedral or octahedral sheets for other ions, without significant change in the layer structure. When a cation in a tetrahedral or octahedral sheet is replaced by a lower valency ion, the substitution leads to an excess of negative charge at the surface of the layer. The most common isomorphous substitutions in clay minerals are Al^{3+} for Si^{4+} in the tetrahedral sheet and Mg^{2+}, Fe^{2+} and Mn^{2+} for Al^{3+} in the octahedral sheet.

  Isomorphous substitutions are common in smectites, which explains their important surface charges compared to other phyllosilicates (Table 2). Depending on the position of the charges, smectites are classified into montmorillonites, whose charges are predominantly in octahedral position, and beidellite, whose charges are predominantly located in tetrahedral position. Bentonites are mainly composed of montmorillonite.

- **Local charges**, which are due to broken bonds and an incomplete neutralization of charges on the edges of the layers. The value of these local charges depends on the pH of the solution [Grunberger, 1995]. In acid environments, charges are positive due to the fixation of H^+ protons on the O^{2-} anions; they are negative if the solution is basic.

  According to Mitchell & Soga [2005], local charges are thought to contribute up to 20% towards the total charge deficit.

		Kaolinite	Illite	Montmorillonite
Surface charges	(meq/100 g)	5–15	20–40	80–100

Table 2: Range of surface charges in kaolinite, illite and montmorillonite [Yong *et al.*, 2009].

The natural tendency is to ensure electroneutrality of the clay particle and therefore, the layer will tend to adsorb cations present in the environment. These cations that form the interlayer are called exchangeable cations as they can be exchanged with other cations of the solution [Van Olphen, 1963]. According to Sposito *et al.* [1984], exchangeable cations are adsorbed at the surface of the layer by at least three different mechanisms:

- **Inner-sphere complexation**, by which cations bind to the clay surface (through primary bonds) without any interposed water molecule.
- **Outer-sphere complexation**, by which solvated cations are attracted and bonded to the clay surface through hydrogen bonds and electrostatic forces.

  Inner-sphere and outer-sphere complexes form the Stern layer [Stern, 1924] (Figure 4). These complexes may be insufficient to balance the negative charges at the clay surface, so that a third mechanism allows to neutralize the residual charges.
- **Electrostatic attraction** of solution cations, resulting from the presence of unbalanced charges at the surface of the clay layer. The attracted cations from the solution form the diffuse double layer (Figure 4).

As mentioned by Sposito *et al.* [1984], outer-sphere complexes differ from cations adsorbed in the diffuse layer in their residence time, i.e. the amount of time that a cation remains adsorbed at a given position. The residence time of cations from the diffuse layer is of the order of 10 ps, which is significantly shorter than the 100 ps residence time of outer-sphere complexes and over 10 ns of inner-sphere complexes (the strongest the bonding, the longest the residence time).

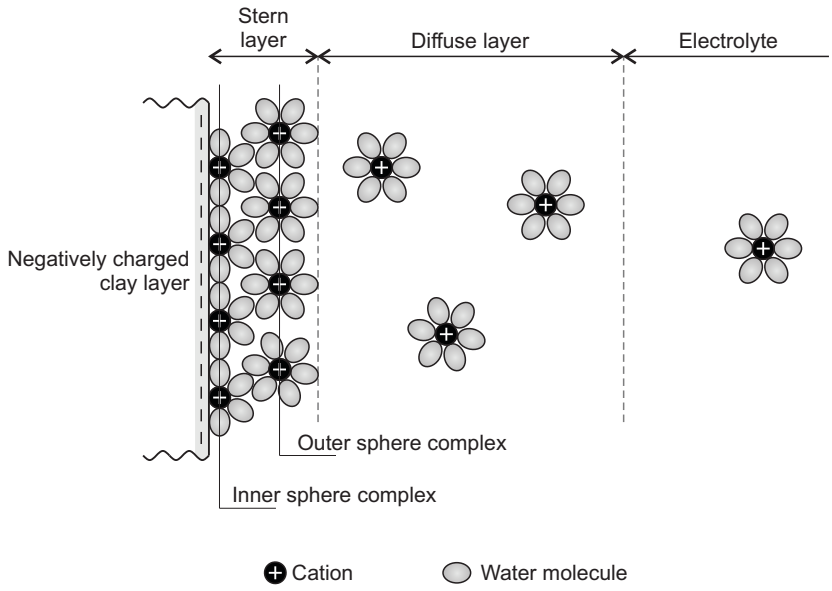

Figure 4: Mechanisms of cation adsorption at the surface of a clay layer [after Meunier, 2005; Yong *et al.*, 2009].

The cation exchange capacity (CEC) measures the ability of smectites to adsorb cations from the solution. The CEC is defined as the number of exchangeable positive charges per 100 g of dry clay mineral. It is expressed in milliequivalents per 100 g of dry clay (meq/100 g). In general, the interlayer comprises a mixture of different cation species, essentially Na^+, Ca^{2+} and Mg^{2+} in bentonites. Table 3 presents the CEC and main exchangeable cations of five reference bentonites. Based on the nature of the dominating exchangeable cations, bentonites are referred to as sodium bentonite or calcium bentonite: Febex and Foca7 are calcium bentonites, GMZ and Kunigel V1 are sodium-calcium bentonites, while MX-80 is a sodium bentonite. As explained in the next section, the nature of the exchangeable cation influences the swelling capacity of the bentonite, with a higher capacity in sodium bentonites.

Finally, another important physicochemical parameter of clay minerals is their specific surface area S_S, expressed in m^2/g. The total specific surface area comprises both the interlayer surface area and the

Bentonite	CEC	Exchangeable cations			Specific surface
		Na^+	Ca^{2+}	Mg^{2+}	
	(meq/100 g)	(meq/100 g)	(meq/100 g)	(meq/100 g)	(m^2/g)
Febex[a]	111	25	47	36	725
FoCa7[b]	69	3	63		454
GMZ[c]	77.3	43	29	12	570–597
Kunigel V1[d]	73	41	29	3	389–687
MX-80[e]	76–88	61–67	8–10	3–5	512–800

[a] Lloret & Villar [2007]
[b] Saiyouri *et al.* [2004]
[c] Wen [2006], Ye *et al.* [2009]
[d] Komine & Ogata [1996], JNC [2000], Marcial *et al.* [2002], Komine [2004]
[e] Pusch [1982], Madsen [1998], Bradbury & Baeyens [2003], Villar [2007]

Table 3: Cation exchange capacity and specific surface of five reference bentonites.

clay particle external surface area. Table 3 presents the values of specific surface area for five reference bentonites. Obviously, a strong correlation of the CEC with the specific surface is observed, the CEC being all the more important that the specific surface is large.

3.3 Hydration and swelling mechanisms in smectites

The swelling capacity of clay minerals refers to their ability to expand upon hydration and shrink upon drying. Accordingly, a good understanding of the hydration mechanisms is required to puzzle out the swelling mechanisms. Starting from dry conditions, two regimes of swelling are generally identified [Norrish, 1954]:

- **Crystalline swelling**, which is predominant at low water contents and corresponds to the progressive intercalation of discrete layers of water in the interlayer space (development of the Stern layer). In the case of smectites, one, two, three or four layers of water molecules are sequentially intercalated, leading the interlayer to increase sequentially from 9.6 Å with no water to 12.6 Å, 15.6 Å, 18.6 Å and 21.6 Å respectively. Figure 5(a) presents the evolution of the interlayer thickness during hydration of compacted MX-80 bentonite.

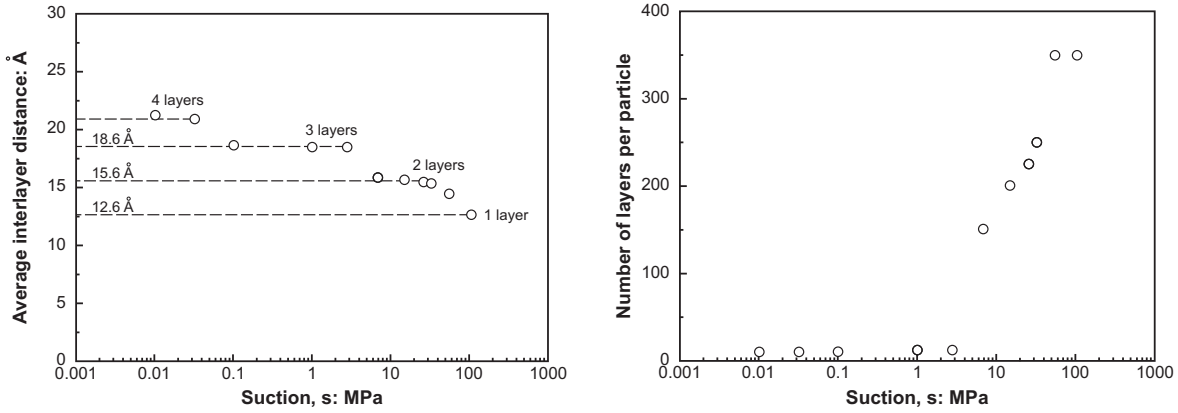

(a) Increase in the number of adsorbed water layers.

(b) Decrease in the number of stacked layers per particle.

Figure 5: Effect of hydration (suction decrease) on particles of MX-80 bentonite [Saiyouri *et al.*, 2004].

As shown in Figure 5(b), the insertion of layers of water molecules in the interlayer space leads to a reorganisation of the solid matrix [Tessier, 1978]. During hydration, clay particles initially made

of 350 layers divide into smaller structures of around 10 layers. These smaller particles are able to fix high amount of water and form water layers up to 100 Å thick [Saiyouri *et al.*, 2000].

- **Osmotic swelling**, which is associated with interactions of the diffuse double layer. Under high water content, the interlayer is a highly concentrated medium as compared with the bulk solution. As a consequence of the difference in cation concentrations, the cations near the clay surface tend to diffuse away. However, the negative electric field at the clay surface prevents the cation to freely diffuse. Contrary to crystalline swelling, swelling is a continuous phenomenon in the osmotic domain. Furthermore, it occurs both between clay layers and between clay particles [Cases *et al.*, 1990; Mitchell & Soga, 2005].

Neglecting the existence of the Stern layer, the clay – water system has traditionally been described using the diffuse double layer (DDL) theory early developed by Gouy [1910] and Chapman [1913]. In the DDL theory, a unique particle surrounded by an ionic solution is considered. The clay layer is supposed uniformly charged over its surface and ions are considered as point charges without interaction. The electrical potential Ψ around the clay layer (Figure 6(a)) is then given by

$$\Psi = \Psi_0 \exp\left(-\kappa x_c\right) \tag{1}$$

where Ψ_0 is the electrical potential at the clay layer surface and x_c is the distance from the clay layer surface. κ^{-1} is the Debye-Hückel length given by

$$\kappa^{-1} = \left(\frac{\varepsilon_r \varepsilon_0 kT}{2n_0 \mathrm{e}^2 z^2}\right)^{1/2} \tag{2}$$

where ε_r is the dielectric constant of the electrolyte, ε_0 is the dielectric permittivity of the vacuum ($= 8.8542 \times 10^{-12}$ C^2/J·m), k is the Boltzmann constant ($= 1.38 \times 10^{-23}$ J/K), T is the absolute temperature, n_0 is the ion concentration in the electrolyte, e is the electric elementary charge ($= 1.602 \times 10^{-19}$ C) and z the valency of the ion in the electrolyte.

The diffuse double layer theory can be used to describe the behaviour of colloidal solutions in which clay minerals are dispersed in a continuous liquid phase [Van Olphen, 1963]. However, in compacted bentonites, the density is such that clay minerals interact through their diffuse double layer and a repulsion force takes place, similarly to two magnets that are brought close to each other. This repulsion force may be assimilated to a swelling pressure (Figure 6(b)). Bolt [1956] used the diffuse double layer theory to predict the swelling pressure developed between two parallel clay layers. Although one can show that this hypothesis is not satisfied in compacted bentonites [see Segad *et al.*, 2010, for a discussion], the theory provides interesting qualitative results. In particular, the repulsive swelling pressure σ_R is expressed as

$$\sigma_R = 2n_0 kT\left(\cosh u - 1\right) \tag{3}$$

where u is a non-dimensional potential at the mid-plane between the two clay layers[2]. This non-dimensional potential u will be all the more important given that the electrical potential Ψ around a single clay layer is large.
Despite the restrictive assumptions behind the double diffuse layer theory, some interesting and qualitative conclusions may be drawn concerning the factors affecting the swelling pressure of bentonite-based materials:

- the higher the dry density, the higher the swelling pressure (Figure 1). Under the assumption of homogeneous and parallel particle distribution, an increase in the dry density yields a decrease in the distance between clay minerals, hence an increase in the mid-plane potential u (Figure 6(b)).
- the higher the CEC, the higher the swelling pressure. A high CEC corresponds to an important surface charge density, hence an important electric potential Ψ_0 and an important mid-plane potential u.
- the lower the valency z of the exchangeable cation, the higher the mid-plane potential u and the higher the swelling pressure. Accordingly, the swelling properties are enhanced for sodium bentonites compared to calcium bentonites.

[2]Details concerning the precise determination of u can be found in Van Olphen [1977] and Tripathy *et al.* [2004].

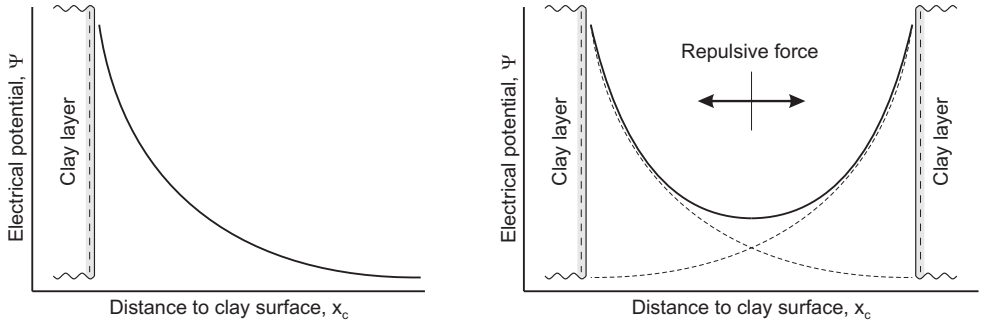

(a) Single clay layer. (b) Two parallel clay layers.

Figure 6: Representation of the double diffuse layer, according to Gouy-Chapman theory. Evolution of the electrical potential as a function of the distance from the clay layer surface.

Analysing in details the mineralogical composition (Table 1), cation exchange capacity and specific surface (Table 3) of the five reference bentonites, the obvious difference in swelling pressure developed by the different materials may be partly explained by the diffuse double layer theory. For instance, one can observe that the low montmorillonite content of Kunigel V1 bentonite is associated with low swelling pressures. Conversely, the important montmorillonite content and Na^+ dominant exchangeable cation of MX-80 bentonite lead to the development of very high swelling pressures upon hydration under constant volume conditions.

4 Structure of compacted bentonites

4.1 Experimental techniques

The microstructure of compacted bentonites[3] can be investigated by using different experimental techniques depending on the type of information required and the scale under consideration. The information that may be obtained from microstructural experimental study includes the pore types, distribution and connectivity, the arrangement and distribution of clay particles and aggregates, the aggregate size and morphology, and the inter-particle contact orientations and contact force directions [Romero & Simms, 2008]. The scale that can be investigated ranges from the nm to the mm. Figure 7 presents the range of applications of five experimental techniques that are commonly used to study the structure of compacted bentonites:

- **Adsorption techniques** are used to determine the specific surface area of clay minerals. Different gases, including nitrogen and carbon dioxide, as well as methylene blue, can be used as sorbates. A description of the different adsorption techniques can be found in Adamson [1990] and Santamarina *et al.* [2002].
- **X-ray diffraction (XRD)** allows the characterization of the mineral phases present in samples. Qualitative and semi-quantitative descriptions of the nature of the clay minerals are possible. The technique may also be used to investigate the effects of the hydration process at the scale of the clay layers [see Cases *et al.*, 1997; Devineau *et al.*, 2006; Likos & Lu, 2006; Villar *et al.*, 2012, among others]. A complete presentation and guide for the interpretation of XRD results are found in Moore & Reynolds [1997].
- **Mercury intrusion porosimetry (MIP)** is a qualitative and quantitative technique used to investigate the pore size distribution (PSD) of a porous sample. The principle is based on the injection of mercury into a sample previously dried. A review of the applications of MIP for the investigation of unsaturated soils microstructure is presented by Romero & Simms [2008].
- **Electron microscopy** provides essentially qualitative information on the pore structure via micrographs of the material, although some quantitative information may be obtained by using digital

[3] In these notes, the term microstructure is used to refer to the structure of materials as observed at a small scale, called microscopic scale, typically ranging from 1 nm to 1 mm.

image analysis. Different techniques exist, such as Scanning Electron Microscopy (SEM), Environmental Scanning Electron Microscopy (ESEM), Transmission Electron Microscopy (TEM). A review of the applications of ESEM for the investigation of unsaturated soils microstructure is presented by Romero & Simms [2008].

- **Computed tomography (CT)**, including microfocus tomography (μCT), is a high-resolution non-destructive 3D observation technique based on the combination of a high number of X-ray images. This class of experimental techniques provides similar information to electron microscopy but in three dimensions.

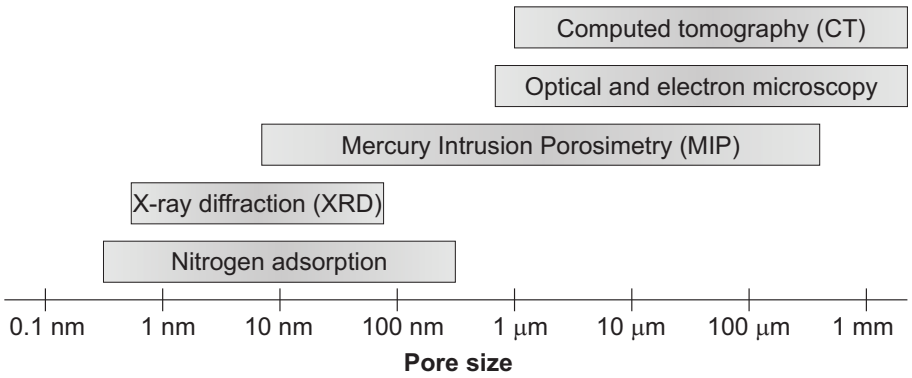

Figure 7: Range of applications of various experimental techniques used to investigate the microstructure of porous materials.

4.2 Experimental observations and representation

Figures 8(a) and 8(b) present ESEM micrographs of compacted Febex and GMZ bentonites respectively. In these micrographs, aggregates with sizes of the order of 20 μm are clearly observed. These aggregates are clusters of clay particles and are formed upon compaction of bentonite dry of optimum. Besides the clay layer and the clay particle, the aggregate represents a third level of organisation in compacted bentonites. Accordingly, the space between aggregates defines a new pore family, called inter-aggregate porosity, or macroporosity.

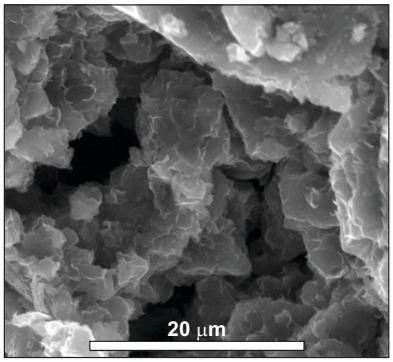

(a) Compacted Febex bentonite with dry density $\rho_d = 1.72$ Mg/m^3 and water content w = 13.7% [Lloret *et al.*, 2003].

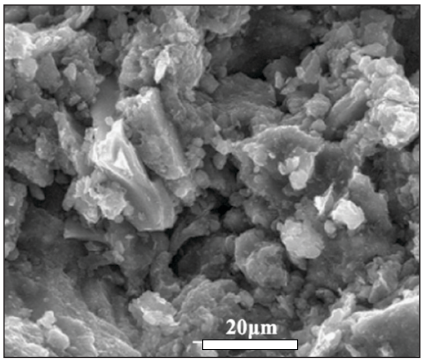

(b) Compacted GMZ bentonite with dry density $\rho_d = 1.75$ Mg/m^3 and water content w = 11.1% [Ye *et al.*, 2009].

Figure 8: Micrographs of two compacted bentonites obtained using an environmental scanning electron microscope.

Mercury intrusion porosimetry provides further insight into the structure of the compacted bentonites and the pore size distribution. Figure 9 presents the pore size distributions obtained by Lloret *et al.* [2003] on Febex bentonite compacted to dry densities of 1.5 Mg/m^3 and 1.8 Mg/m^3. In this figure, a bimodal distribution is clearly observed, the two peaks being in the range of pore sizes of 10 nm and 10 μm for

the highest dry density, and 10 nm and 40 μm for the lowest dry density. The size of the larger pores is consistent with the inter-aggregate pores observed in Figure 8(a).

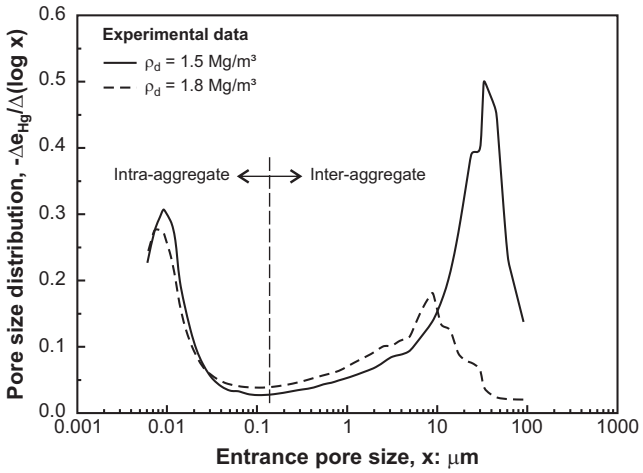

Figure 9: Pore size distribution of Febex bentonite compacted at different dry densities, $\rho_d = 1.5$ Mg/m^3 and $\rho_d = 1.8$ Mg/m^3 [Lloret *et al.*, 2003].

In Figure 9, the pore family with the peak around 10 nm corresponds to the intra-aggregate porosity, and more specifically the inter-particle porosity. Note that pores smaller than around 6 nm (corresponding essentially to intra-particle pores) cannot be investigated by using mercury intrusion porosimetry. The intra-aggregate porosity is therefore not homogeneous and includes pores between particles (inter-particle porosity) and inside a particle (inter-layer porosity). In the following, the term microporosity is used to refer to the total intra-aggregate porosity.

4.3 Water storage and hydration mechanisms

Water in compacted bentonite is present under different forms: structural water, adsorbed water and capillary or free water [Kezdi, 1974; Stçepkowska, 1990]. Structural water or hydroxyl is part of the minerals structure and does not leave the solid phase below 350°C. It is therefore excluded from water content measurements which are obtained after drying the sample at a temperature slightly over 100°C. Adsorbed water corresponds to the water which is adsorbed on both internal and external surfaces of the clay minerals, i.e. which is stored in the intra-aggregate pores (micropores). Finally, capillary or free water is stored in the macropores. Figure 10 presents a conceptual representation of the structure of compacted bentonites and the different types of water.

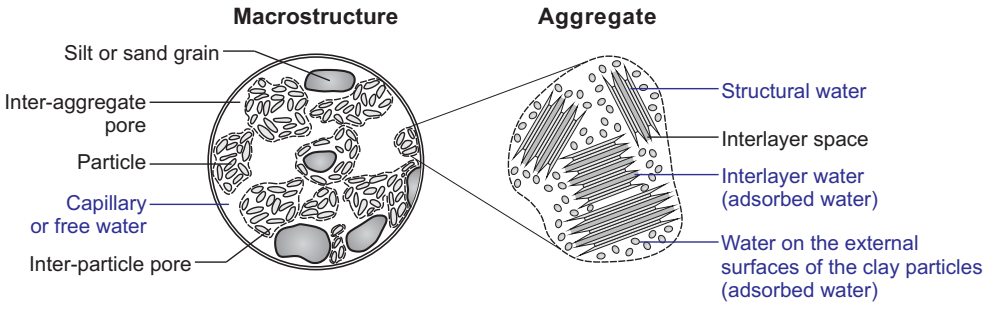

Figure 10: Conceptual representation of the structure of compacted bentonite (in black) and the different water storage mechanisms (in blue) [modified after Gens & Alonso, 1992; Jacinto *et al.*, 2012].

The physical state of water in the vicinity of the charged clay layers differs from the one of bulk water, and both values of viscosity and density are affected [Langmuir, 1917; Baver & Winterkorn, 1935; Winterkorn, 1943]. Low [1979] and Bourg *et al.* [2003] showed that the viscosity of the adsorbed water is higher than the one of bulk water. Moreover, due to the strong physicochemical interactions between water and the clay particles, the density of adsorbed water is significantly higher than that of bulk water [Hawkins & Egelstaff, 1980; Derjaguin *et al.*, 1986; Swenson *et al.*, 2000; Jacinto *et al.*, 2012], and may reach values higher than 1.4 Mg/m^3 (Figure 11(a)).

From a practical point of view, the water density has a strong influence on the computed degree of saturation. The degree of saturation S_r is indeed obtained from the gravimetric water content w according to

$$S_r = \frac{\rho_s}{\rho_w}\frac{w}{e} \tag{4}$$

where ρ_s is the density of the solids, ρ_w is the water density and e is the void ratio (defined as the ratio between the volume of voids and the volume of solids). When the degree of saturation is calculated with the density of bulk water ($\rho_w = 1$ Mg/m^3), values higher than 1 are systematically obtained close to saturation [Villar, 2002; Marcial, 2003; Jacinto *et al.*, 2012]. Knowing the water content and void ratio of presumably saturated samples, Villar [2000] computed the equivalent water density in compacted Febex bentonite. Figure 11(b) shows that the mean water density is higher for denser samples, although water densities higher than 1 are found for looser samples.

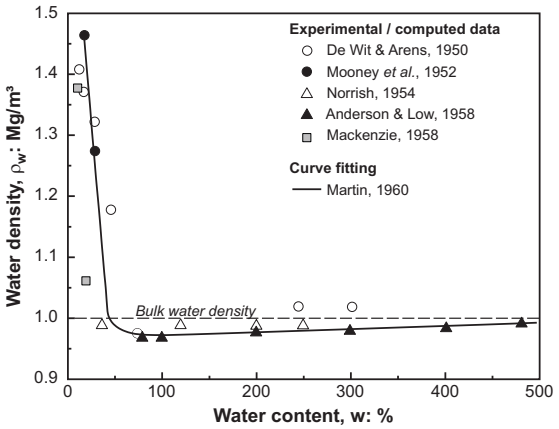

(a) Water density in sodium montmorillonite as a function of water content [Martin, 1960].

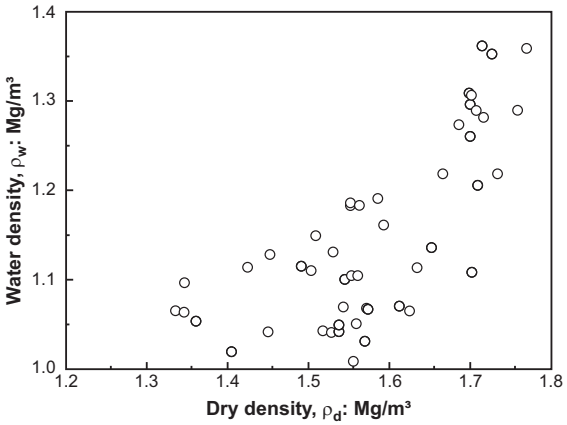

(b) Water density in Febex bentonite as a function of dry density [Villar, 2000].

Figure 11: Water density in compacted bentonites.

In practice, the different types of water cannot be easily separated. Thermogravimetric analysis is generally used to this end, although the interpretation of the results is not straightforward [Cases *et al.*, 1997, 1995; Salles *et al.*, 2009]. At relative humidities lower than 90%, water is mainly found in the interlayer and adsorbed on the external surface of the particles. When the relative humidity increases, some capillary condensation is believed to take place in the macropores. However, as discussed in the next section, important porosity redistribution occurs upon wetting and leads a reduction of the macroporosity under confined conditions, hence limiting the amount of free water. The amount of free water in compacted bentonites is therefore usually estimated to be only a few percent of the total water, under saturated conditions [Pusch *et al.*, 1990; Bradbury & Baeyens, 2003; Fernandez *et al.*, 2004].

4.4 Factors affecting the structure

The mechanisms affecting the structure of soils may be classified into internal and external factors. Internal factors (also called intrinsic) include the mineralogy, clay particles size and morphology, and water chemistry. External factors are the compaction method and its energy, and the water content. In this section, the structure evolution is only considered from the point of view of the pore size distribution, as little information is available about the morphology of the pores and aggregates structure.

4.4.1 Mechanical loading

Figure 9 presents the pore size distributions of Febex bentonite compacted at two different dry densities, namely 1.5 Mg/m^3 and 1.8 Mg/m^3, but the same water content. In both cases, a bimodal pore size distribution is observed, even at high dry density. The compaction process has two main effects. Firstly, regarding the porous volume, increasing the compaction effort at constant water content decreases the volume of macropores, while the volume of micropores is hardly affected. Secondly, compaction shifts the size of dominant macropores towards smaller pore radii.

4.4.2 Water content changes

As a result of the sensitivity of clay minerals to water, the structure of compacted bentonites is significantly affected by changes in water content. An increase in the water content leads indeed to the swelling of clay layers and particles, hence aggregates. Figure 12 shows the evolution of the pore size distribution of MX-80 bentonite compacted to a dry density of 1.79 Mg/m^3 and hydrated under constant volume conditions. The experimental data show an increase of volume of the smaller pores and a progressive decrease of the inter-aggregate pore volume. Consequently, the structure of the material evolves from a bimodal pore size distribution (as-compacted material) towards a mono-modal distribution under fully saturated conditions. According to Romero [2013], the evolution of the macropores volume upon changes in water content is the consequence of both multi-scale and multi-physical processes. During wetting, the expanding clay particles invade indeed the macropores, hence decreasing the macropores volumes. On the other hand, wetting is likely to lead to collapse of the macrostructure. At the macroscopic scale, collapse is indeed often detected during saturation of compacted bentonites and is generally interpreted as an instability of the material structure.

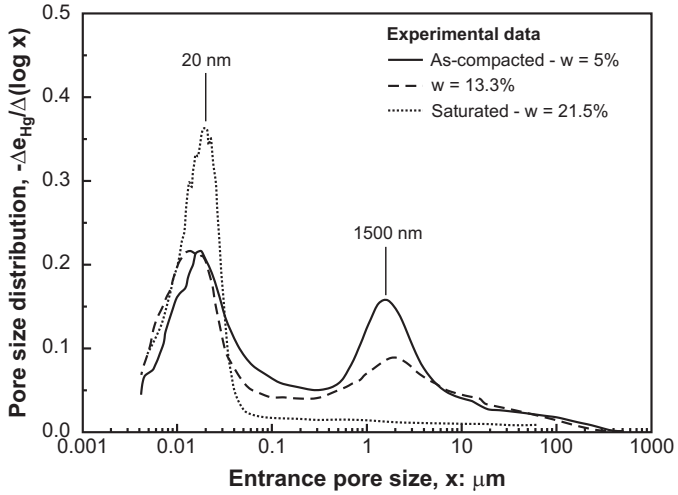

Figure 12: Influence of the water content on the pore size distribution of MX-80 bentonite compacted to a dry density $\rho_d = 1.79$ Mg/m^3 and hydrated under constant volume conditions [Seiphoori *et al.*, 2014]

Figure 13 presents an interesting picture, obtained by cryo-Focused Ion Beam nanotomography [see Keller *et al.*, 2014, for details on this technique], of partially saturated MX-80 bentonite compacted to a dry density of 1.46 Mg/m^3 with a water content of 22.6%. The picture shows that the inter-aggregate pores are filled with a loose material comparable to a gel or colloidal solution. This material is characterized by a special structures referred to as honeycomb [Keller *et al.*, 2014]. For higher dry densities (1.67 Mg/m^3), Keller *et al.* [2014] did not observe such a structure, presumably because of the lack of large inter-aggregate pores (Figure 12).
Wang *et al.* [2013a] observed a different behaviour of the microstructure of a MX-80 bentonite/sand mixture hydrated under confined conditions, and noticed the development of two-dimensional fissure-like pores. These pores were detected with both mercury intrusion porosimetry (pore group with a mean diameter of 50 μm and 1 μm in Figure 14(a)) and scanning environmental microscope (Figure 14(b)). Wang *et al.* [2013a] suggested that these pores may result from the division of clay particles within the aggregates due to swelling. However, further investigations are required since the release of the swelling pressure before freeze-drying of the sample could also influence the observations.

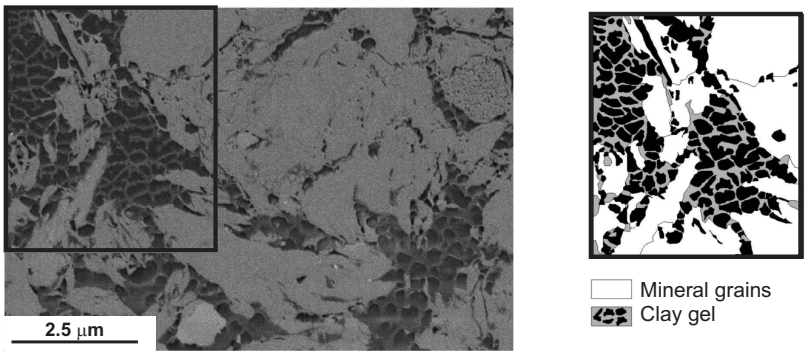

Figure 13: Microstructure of compacted MX-80 bentonite with dry density $\rho_d = 1.46$ Mg/m^3 and water content $w = 22.6\%$ obtained by cryo-Focused Ion Beam nanotomography [Keller *et al.*, 2014].

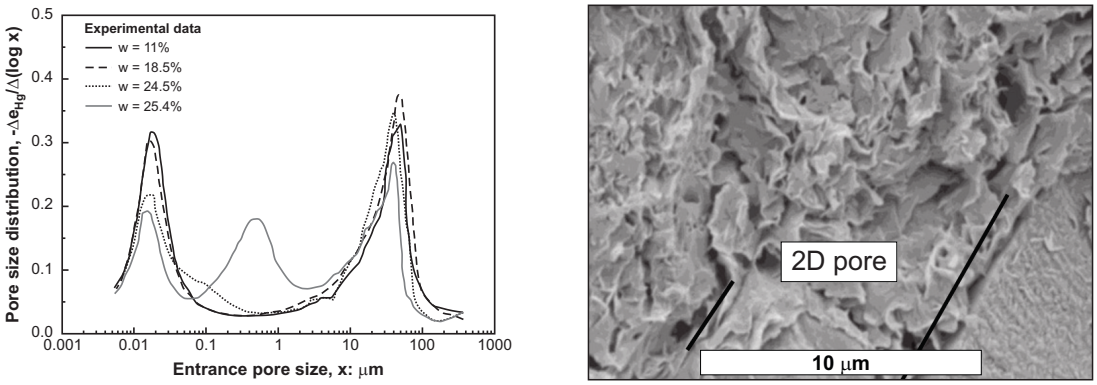

(a) Evolution of the pore size distribution.

(b) Micrograph for saturated conditions ($w = 25.5\%$).

Figure 14: Development of two-dimensional fissure like pores during hydration of a MX-80 bentonite/sand mixture under constant volume conditions [Wang *et al.*, 2013a]

Finally, few experimental data are available concerning the reversibility of the microstructure behaviour upon wetting and drying cycles. According to Romero [2013], the aggregates of as-compacted bentonites swell and shrink almost reversibly upon wetting and drying. Therefore Romero [2013] qualifies the aggregates of compacted clayey soils as a permanent feature of the microstructure. However, Seiphoori *et al.* [2014] observed significant and permanent modifications of the structure of granular MX-80 bentonite saturated under constant volume conditions. Indeed, no significant structural changes were observed upon drying. Seiphoori *et al.* [2014] interpreted this irreversibility of the structure behaviour as a consequence of the irreversible subdivision of smectite particles (see Section 3.3).

4.4.3 Ageing

Ageing effects refer to time-dependent phenomena. These effects were studied by Delage *et al.* [2006] on MX-80 bentonite (Figure 15). The study showed that significant changes in the material structure were observed when bentonite samples were maintained under constant volume and constant water content for different periods of time ranging from 1 day to 90 days. In particular, a decrease in the inter-aggregate porosity and an increase in the non-intruded porosity (interpreted as inter-layer porosity) were observed. These observations were interpreted in terms of progressive placement of interlayer water molecules within the particles and subdivision of clay particles.

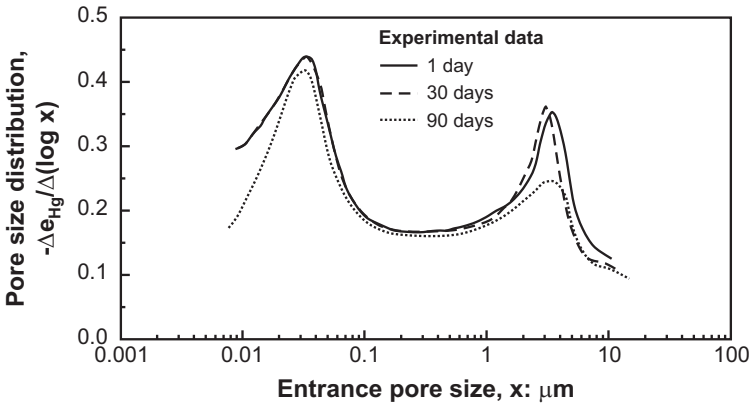

Figure 15: Changes in pore size distribution with time of compacted MX-80 bentonite with dry density $\rho_d = 1.61$ Mg/m^3 and water content $w = 8.2$% [Delage *et al.*, 2006].

4.5 Model for the microstructure evolution

In the previous section, the effects of hydraulic and mechanical loading on the microstructure of compacted bentonites were underlined. In particular, the experimental observations showed that the microstructure of compacted bentonites created upon compaction was not fixed, but evolving along hydromechanical stress paths. In this section, attention is focused on quantifying the evolution of the microstructure.

The experimental technique the most often used to gather quantitative information on the structure of porous media is mercury intrusion porosimetry. While the technique provides only partial information on the material microstructure, the results can be used to obtain a scalar measure of the interconnected pore sizes and volumes. Accounting for this limitation, mercury intrusion porosimetry data are often used and analysed in order to highlight tendencies in the evolution of the pore size distribution of compacted bentonites along hydromechanical stress paths [Romero *et al.*, 2011; Della Vecchia *et al.*, 2015]. In particular, the following quantities are defined:

- the **microporosity** ϕ_m is the ratio between the micropores volume Ω_m and the total volume Ω

$$\phi_m = \frac{\Omega_m}{\Omega}. \tag{5}$$

  The microporosity coincides with the total intra-aggregate porosity and includes both inter- and intra-particles pores.

- the **microstructural void ratio** e_m is the ratio between the micropores volume Ω_m and the solid volume Ω_s

$$e_m = \frac{\Omega_m}{\Omega_s} = \frac{\phi_m}{\phi} e \tag{6}$$

  where ϕ and e are respectively the (total) porosity and void ratio.

- the **macroporosity** ϕ_M is the ratio between the macropores volume Ω_M and the total volume Ω

$$\phi_M = \frac{\Omega_M}{\Omega}. \tag{7}$$

  The macroporosity coincides with the inter-aggregate porosity.

- the **macrostructural void ratio** e_M is the ratio between the macropores volume Ω_M and the solid volume Ω_s

$$e_M = \frac{\Omega_M}{\Omega_s} = \frac{\phi_M}{\phi} e \tag{8}$$

  with the total porosity $\phi = \phi_m + \phi_M$ and total void ratio $e = e_m + e_M$.

From a practical point of view, these quantities can be estimated based on experimental pore size distributions. Therefore a criterion should be defined to distinguish micropores from macropores. Three main approaches are identified and briefly summarized:

- **Approach 1**: an entrance pore size is selected based on the pore size distribution of the as-compacted material and is used to separate intra-aggregate and inter-aggregate pores.
- **Approach 2**: data from a mercury intrusion and extrusion cycles are used. The difference between the intruded and extruded mercury volume is assumed to correspond to the inter-aggregate porosity [Delage & Lefebvre, 1984; Delage *et al.*, 1996].
- **Approach 3**: the entrance pore size coinciding with the dominant peak of the pore size distribution of the material saturated under constant volume conditions is detected. It is used to separate intra-aggregate and inter-aggregate pores [Della Vecchia, 2009; Romero *et al.*, 2011].

The different criteria are further described and discussed in Romero *et al.* [2011]. In addition, a fourth approach, based on the discrimination of water retention domains, was proposed by Romero *et al.* [1999]. Yet, if the approaches are conceptually different, they generally provide similar quantitative results in terms of porosities evolution.

Based on the experimental observations presented in the previous section, two main conclusions can be drawn. Firstly, mechanical loading does not affect the volume of micropores. This is at least true for the range of loads and dry densities commonly investigated. Secondly, hydraulic loading strongly affects the micropores volume. In particular, wetting yields an increase of the micropores volume. Accordingly, Romero *et al.* [2011] suggested to plot the microstructural void ratio e_m obtained from the analysis of pore size distributions as a function of the water ratio e_w (defined as the ratio between the volume of water and the volume of solids). By doing so, Romero *et al.* [2011] and Della Vecchia *et al.* [2013] observed that, below a given water ratio $e_w = e_m^*$, the microstructural void ratio of moderately active clays was almost constant and not affected by the water ratio. On the contrary, for higher water ratios, the microstructural void ratio increases almost linearly with the water ratio. Therefore, Romero *et al.* [2011] and Della Vecchia *et al.* [2013] proposed the following law for the evolution of the microstructural void ratio with the water ratio

$$e_m = e_m^* + \beta \langle e_w - e_m^* \rangle \tag{9}$$

where $\langle\rangle$ designates the Macaulay brackets (ramp function), e_m^* is the water ratio corresponding to fully saturated micropores and β quantifies the swelling tendency of the aggregates.

Dieudonné *et al.* [2013], Della Vecchia *et al.* [2015] and Dieudonné *et al.* [2017] analysed a large number of mercury intrusion porosimetry results on different bentonites. The materials include Febex bentonite [Lloret *et al.*, 2003; Lloret & Villar, 2007; Romero *et al.*, 2011], Kunigel V1 bentonite [Romero, 2012, and present work], MX-80 bentonite [Delage *et al.*, 2006; Wang, 2012; Seiphoori *et al.*, 2014] and a mixture of MX-80 bentonite and sand [Wang *et al.*, 2013b; Saba *et al.*, 2014]. The analysis of the experimental results and their representation in the $(e_w - e_m)$ plane does not allow identifying any threshold water content below which the microstructural water ratio remains constant. On the contrary, the micropores volume appears to be continuously evolving with the water ratio (Figure 16). This observation is in accordance with results presented by Romero *et al.* [2011] on Febex and MX-80 bentonites.

Accordingly, Dieudonné *et al.* [2013] proposed to describe the evolution of microstructural void ratio with the water ratio

$$e_m = e_{m0} + \beta_0 e_w + \beta_1 e_w^2 \tag{10}$$

where e_{m0} is the microstructural void ratio for the dry material ($e_w = 0$) and β_0 and β_1 are parameters that quantify the swelling potential of the aggregates. Table 4 presents the model parameters calibrated for four bentonite-based materials, namely Febex, Kunigel V1 and MX-80 bentonites, and a mixture of MX-80 bentonite and sand. In particular, Figure 16 provides an example of the calibration for MX-80 bentonite, using experimental data from Delage *et al.* [2006], Seiphoori *et al.* [2014] and Wang *et al.* [2014].

Three remarks are formulated concerning the proposed model. First of all, it should be noted that for high values of dry density and water content, Equation (10) may lead to values of e_m higher than the total void ratio e. In this case, it is assumed that the microstructure is completely developed and $e_m = e$. This remark is directly related to the fact that Equation (10) does not provide any limiting value of e_m with e_w, although such a limit probably exists. However, the proposed relation is meant to describe the microstructure of compacted bentonites for which the range of water ratios is limited to $0.15 \preceq e_w \preceq 0.95$. Finally, in a reasonable range of water ratios, Equation (10) provides predictions similar to those of the

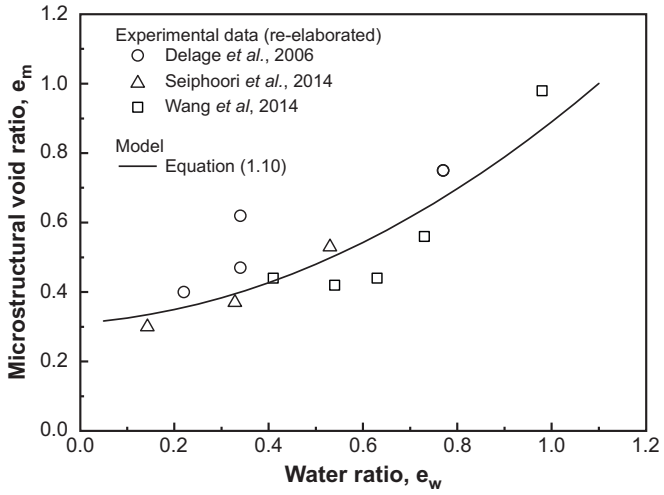

Figure 16: Evolution of the microstructural void ratio e_m with the water ratio e_w from MIP results on compacted MX-80 bentonite.

Material	e_{m0}	β_0	β_1
Febex	0.35	0.25	0.15
Kunigel V1	0.4	0.03	0.21
MX-80	0.31	0.1	0.48
MX-80/sand mixture (70/30)	0.29	0.1	0.18

Table 4: Parameters of the microstructure evolution law for four bentonite-based materials.

bilinear expression proposed by Romero *et al.* [2011], whilst providing a continuous evolution of e_m with the water ratio.

5 Summary

Bentonites exhibit a complex behaviour under repository conditions, owing to the high sensitivity of the material to mechanical and environmental (thermal, hydraulic and pneumatic) loads. This sensitivity of bentonites to external factors arises from both the mineralogical composition and the multi-scale structure of the material, which can be investigated by using modern experimental techniques.

In these lecture notes, attention was first focused on the physicochemical properties of smectites and the hydration and swelling mechanisms of these minerals. At the scale of the clay particle, hydration leads to an increase of the average interlayer distance and a division of the clay particles into smaller structures, both contributing to the particle swelling. A precise description of the processes is complex. Yet, the diffuse double layer theory provides interesting qualitative results on the factors affecting swelling. In particular, the theory allows a first explanation of the considerably different swelling pressures reached by different bentonites upon saturation.

The hydration and swelling mechanisms were then addressed at the scale of the compacted material microstructure. The experimental data show that hydration of compacted bentonite under confined conditions is associated with a progressive increase of the micropores volume and a decrease of the inter-aggregate porosity. On the contrary, under unconfined conditions, swelling taking place at the clay layer yields important swelling strains observed at the macroscopic scale. Based on the interpretation of a large number of pore size distributions on compacted bentonites, a model for the microstructure evolution is proposed.

References

Adamson, A. W. (1990). *Physical chemistry of surfaces*. John Wiley & Sons.

Anderson, D. M. & Low, P. F. (1958). The density of water adsorbed by Li-, Na-, and K-bentonite. *Soil Science Society of America Proceedings* **22**, 99–103.

Apted, M. (1995). The scientific and regulatory basis for the geological disposal of radioactive waste. In *Repository and barrier concepts* (Savage, D., Ed.), Wiley.

Baver, L. D. & Winterkorn, H. W. (1935). Sorption of liquids by soil colloids: II. Surface behaviour in the hydration of clays. *Soil Science* **40**, No. 5, 403–418.

Bolt, G. H. (1956). Physico-chemical analysis of the compressibility of pure clays. *Géotechnique* **6**, No. 2, 86–93.

Bourg, I. C., Bourg, A. C. M. & Sposito, G. (2003). Modeling diffusion and adsorption in compacted bentonite: a critical review. *Journal of Contaminant Hydrology* **61**, No. 1–4, 293–302.

Bradbury, M. H. & Baeyens, B. (2003). Porewater chemistry in compacted re-saturated MX-80 bentonite. *Journal of Contaminant Hydrology* **61**, No. 1–4, 329–338.

Bruno, G. (1993). *Etude expérimentale des mécanismes de reduction et d'oxydation du Fer d'une argile naturelle – Evolution de ses propriétés physiques et chimiques*. Ph.D. thesis, Université de Poitiers.

Börgesson, L., Karnland, O. & Johannesson, L. E. (1996). Modelling of the physical behaviour of clay barriers close to water saturation. *Engineering Geology* **41**, No. 1–4, 127–144.

Cases, J. M., Berend, I., Besson, G., Francois, M., Uriot, J. P., Thomas, F. & Poirier, J. E. (1995). Mechanism of adsorption and desorption of water vapor by homoionic montmorillonites: 2. The Li^+, Na^+, K^+, Rb^+ and Cs^+- exchanged forms. *Clays and Clay Minerals* **43**, No. 3, 324–336.

Cases, J. M., Berend, I., Delon, J. F., François, M., Grillet, Y., Michot, I., Poirier, J. E. & Yvon, J. (1990). Quelques aspects de l'étude des propriétés texturales des argiles. In *Matériaux argileux: structure, propriétés et applications, Société Française de Minéralogie, Groupe français des argiles* (Decarreau, A., Ed.), pp. 309–342.

Cases, J. M., Berend, I., Francois, M., Uriot, J. P., Michot, L. J. & Thomas, F. (1997). Mechanism of adsorption and desorption of water vapor by homoionic montmorillonite. 3. The Mg^{2+}, Ca^{2+}, and Ba^{2+} exchanged forms. *Clays and Clay Minerals* **45**, No. 1, 8–22.

Chapman, D. L. (1913). A contribution to the theory of electro-capillarity. *Physiological Magazine* **25**, No. 6, 475–481.

De Wit, C. T. & Arens, P. L. (1950). Moisture content and density of some clay minerals and some remarks on the hydration pattern of clay. In *Proceeding of the Fourth International Congress of Soil Sciences*, pp. 59–62.

Delage, P., Audiguier, M., Cui, Y. & Howat, M. (1996). Microstructure of a compacted silt. *Canadian Geotechnical Journal* **33**, No. 1, 150–158.

Delage, P. & Lefebvre, G. (1984). Study of the structure of a sensitive Champlain clay and of its evolution during consolidation. *Canadian Geotechnical Journal* **21**, No. 1, 21–35.

Delage, P., Marcial, D., Cui, Y. J. & Ruiz, X. (2006). Ageing effects in a compacted bentonite: a microstructure approach. *Géotechnique* **56**, No. 5, 291–304.

Della Vecchia, G. (2009). *Coupled hydro-mechanical behaviour of compacted clayey soils*. Ph.D. thesis, Politecnico di Milano.

Della Vecchia, G., Dieudonne, A. C., Jommi, C. & Charlier, R. (2015). Accounting for evolving pore size distribution in water retention models for compacted clays. *International Journal for Numerical and Analytical Methods in Geomechanics* **39**, No. 7, 702–723.

Della Vecchia, G., Jommi, C. & Romero, E. (2013). A fully coupled elastic–plastic hydromechanical model for compacted soils accounting for clay activity. *International Journal for Numerical and Analytical Methods in Geomechanics* **37**, No. 5, 503–535.

Derjaguin, B. V., Karasev, V. V. & Khromova, E. N. (1986). Thermal expansion of water in fine pores. *Journal of Colloid and Interface Science* **109**, No. 2, 586–587.

Devineau, K., Bihannic, I., Michot, L., Villiéras, F., Masrouri, F., Cuisinier, O., Fragneto, G. & Michau, N. (2006). In situ neutron diffraction analysis of the influence of geometric confinement on crystalline swelling of montmorillonite. *Applied Clay Science* **31**, No. 1–2, 76–84.

Dieudonné, A. C., Della Vecchia, G. & Charlier, R. (2017). Water retention model for compacted bentonites. *Canadian Geotechnical Journal* **54**, 915–925.

Dieudonné, A. C., Levasseur, S., Charlier, R., Della Vecchia, G. & Jommi, C. (2013). A water retention model for compacted clayey soils. In *Computational Geomechanics*, Cracow, Poland, pp. 23–31.

Dixon, D. A., Gray, M. N. & Graham, J. (1996). Swelling and hydraulic properties of bentonites from Japan, Canada and the USA. *Environmental Geotechnics* **1**, 43–48.

Fernandez, A. M. (2004). *Caracterización y modelización del agua intersticial en materiales arcillosos: estudio de la bentonita de Cortijo de Archidona*. Ph.D. thesis, CIEMAT.

Fernandez, A. M., Baeyens, B., M., B. & Rivas, P. (2004). Analysis of the pore water chemical composition of a spanish compacted bentonite used in an engineered barrier. *Physics and Chemistry of the Earth* **29**, No. 1, 105–118.

Gens, A. & Alonso, E. E. (1992). A framework for the behaviour of unsaturated expansive clays. *Canadian Geotechnical Journal* **29**, No. 6, 1013–1032.

Gens, A., Vallejan, B., Sánchez, M., Imbert, C., Villar, M. V. & Van Geet, M. (2011). Hydromechanical behaviour of a heterogeneous compacted soil: experimental observations and modelling. *Géotechnique* **61**, No. 5, 367–386.

Gouy, M. (1910). Sur la constitution de la charge électrique à la surface d'un électrolyte. *Journal de Physique Théorique et Appliquée* **9**, No. 1, 457–468.

Grim, R. E. (1968). *Clay mineralogy*. New-York, USA: McGraw-Hill.

Grunberger, D. (1995). *Etude expérimentale de l'évolution des microstructures et des propriétés physiques et mécaniques des argiles au cours de la compaction*. Ph.D. thesis, Université de Montpellier II.

Hawkins, R. K. & Egelstaff, P. A. (1980). Interfacial water structure in montmorillonite from neutron diffraction experiments. *Clays and Clay Minerals* **28**, No. 1, 19–28.

Hewitt, D. F. (1917). The origin of bentonites. *Washington Academy of Sciences Journal* **7**, 196–198.

Jacinto, A. C., Villar, M. V. & Ledesma, A. (2012). Influence of water density on the water-retention curve of expansive clays. *Géotechnique* **62**, No. 8, 657–667.

JNC (2000). H12 project to establish technical basis for HLW disposal in Japan. Supporting report 3: safety assessment of the geological disposal system. *Technical report*, Japan Nuclear Cycle Developement Institute.

Karnland, O., Nilsson, U., Weber, H. & Wersin, P. (2008). Sealing ability of Wyoming bentonite pellets foreseen as buffer material – Laboratory results. *Physics and Chemistry of the Earth* **33**, 472–475.

Keller, L. M., Seiphoori, A., Gasser, P., Lucas, F., Holzer, L. & Ferrari, A. (2014). The pore structure of compacted and partly saturated MX-80 bentonite at different dry densities. *Clays and Clay Minerals* **62**, No. 3, 174–187.

Kezdi, A. (1974). *Handbook of soil mechanics. Soil physics*. Elsevier Scientific.

Knight, W. C. (1898). Bentonite. *Engineering and Mining Journal* **66**, 491.

Komine, H. (2004). Simplified evaluation on hydraulic conductivities of sand–bentonite mixture backfill. *Applied Clay Science* **26**, No. 1–4, 13–19.

Komine, H. & Ogata, N. (1996). Prediction for swelling characteristics of compacted bentonite. *Canadian Geotechnical Journal* **33**, No. 1, 11–22.

Lajudie, A., Raynal, J., Petit, J. C. & Toulhoat, P. (1994). Clay-based materials for engineered barriers: a review. *Materials Research Society Symposium Proceedings* **353**, 221–229.

Langmuir, I. (1917). The constitution and fundamental properties of solids and liquids. *Journal of the American Chemical Society* **39**, 1848–1906.

Likos, W. J. & Lu, N. (2006). Pore-scale analysis of bulk volume change from crystalline interlayer swelling in Na^{+}- and Ca^{2+}-smectite. *Clays and Clay Minerals* **54**, No. 4, 515–528.

Lloret, A. & Villar, M. V. (2007). Advances on the knowledge of the thermo-hydro-mechanical behaviour of heavily compacted FEBEX bentonite. *Physics and Chemistry of the Earth* **32**, No. 8–14, 701–715.

Lloret, A., Villar, M. V., Sánchez, M., Gens, A., Pintado, X. & Alonso, E. E. (2003). Mechanical behaviour of heavily compacted bentonite under high suction changes. *Géotechnique* **53**, No. 1, 27–40.

Low, P. F. (1979). Nature and properties of water in montmorillonite-water systems. *Soil Science Society of America Journal* **43**, No. 4, 651–658.

Mackenzie, R. C. (1958). Density of water sorbed on montmorillonite. *Nature* **181**, 334.

Madsen, F. T. (1998). Clay mineralogical investigations related to nuclear waste disposal. *Clay Minerals* **33**, No. 1, 109–129.

Marcial, D. (2003). *Comportement hydromécanique et microstructural des matériaux de barrière ouvragée*. Ph.D. thesis, Ecole Nationale des Ponts et Chaussées.

Marcial, D., Delage, P. & Cui, Y. J. (2002). On the high stress compression of bentonites. *Canadian Geotechnical Journal* **39**, No. 4, 812–820.

Martin, T. R. (1960). Adsorbed water on clay: a review. *Clays and Clay Minerals* **9**, No. 1, 28–70.

Meunier, A. (2005). *Clays*. Springer.

Mitchell, J. K. & Soga, K. (2005). *Fundamentals of soil behaviour*. Wiley.

Montes-H, G. (2002). *Etude expérimentale de la sorption d'eau et du gonflement des argiles par microscopie électronique à balayage environnementale (ESEM)*. Ph.D. thesis, Université Louis Pasteur.

Mooney, R. W., Keenan, A. G. & Wood, L. A. (1952). Adsorption of water vapor by montmorillonite. II. Effect of exchangeable ions and lattice swelling as measured by X-ray diffraction. *Journal of the American Chemical Society* **74**, No. 6, 1371–1374.

Moore, D. M. & Reynolds, R. C. (1997). *X-ray diffraction and the identification and analysis of clay minerals*. Oxford University Press.

Nakashima, Y. (2004). Nuclear magnetic resonance properties of water-rich gels of Kunigel-V1 bentonite. *Journal of Nuclear Science and Technology* **41**, No. 10, 981–992.

Norrish, K. (1954). The swelling of montmorillonite. *Discussions of the Faraday Society* **18**, 120–134.

Proust, D., Lechelle, J., Lajudie, A. & Meunier, A. (1990). Hydrothermal reactivity of mixed-layer kaolinite/smectite: experimental transformation of high-charge to low-charge smectite **38**, No. 4, 415–425.

Pusch, R. (1982). Mineral-water interactions and their influence on the physical behavior of highly compacted Na bentonite. *Canadian Geotechnical Journal* **19**, No. 3, 381–387.

Pusch, R., Karnland, O. & Hokmark, H. (1990). GMM - a general microstructural model for qualitative and quantitative studies of smectite clays. *Technical report*, SKB.

Romero, E. (2012). Complementary triaxial compression and direct shear tests under high matric suctions on low-density Kunigel V1. *Technical report*, Universitat Politecnica de Catalunya.

Romero, E. (2013). A microstructural insight into compacted clayey soils and their hydraulic properties. *Engineering Geology* **165**, 3–19.

Romero, E., Della Vecchia, G. & Jommi, C. (2011). An insight into the water retention properties of compacted clayey soils. *Géotechnique* **61**, No. 4, 313–328.

Romero, E., Gens, A. & Lloret, A. (1999). Water permeability, water retention and microstructure of unsaturated compacted Boom clay. *Engineering Geology* **54**, No. 1–2, 117–127.

Romero, E. & Simms, P. H. (2008). Microstructure investigation in unsaturated soils: a review with special attention to contribution of mercury intrusion porosimetry and environmental scanning electron microscopy. *Geotechnical and Geological Engineering* **26**, No. 6, 705–727.

Ross, C. S. & Shannon, E. V. (1926). The minerals of bentonite and related clays and their physical properties. *Journal of the American Ceramic Society* **9**, No. 2, 77–96.

Saba, S., Delage, P., Lenoir, N., Cui, Y. J., Tang, A. M. & Barnichon, J. D. (2014). Further insight into the microstructure of compacted bentonite-sand mixture. *Engineering Geology* **168**, 141–148.

Saiyouri, N., Hicher, P. Y. & Tessier, D. (2000). Microstructural approach and transfer water modelling in highly compacted unsaturated swelling clays. *Mechanics of Cohesive-Frictional Materials* **5**, 41–60.

Saiyouri, N., Tessier, D. & Hicher, P. Y. (2004). Experimental study of swelling in unsaturated compacted clays. *Clay Minerals* **39**, 469–479.

Salles, F., Douillard, J. M., Denoyel, R., Bildstein, O., Jullien, M., Beurroies, I. & Van Damme, H. (2009). Hydration sequence of swelling clays: evolutions of specific surface area and hydration energy. *Journal of Colloid and Interface Science* **333**, No. 2, 510–522.

Santamarina, J. C., Klein, W. Y. H., K. A. & Prencke, E. (2002). Specific surface: determination and relevance. *Canadian Geotechnical Journal* **39**, No. 1, 233–241.

Schanz, T. & Al-Badran, Y. (2014). Swelling pressure characteristics of compacted Chinese Gaomiaozi bentonite GMZ01. *Soils and Foundations* **54**, No. 4, 748–759.

Segad, M., Jönsson, B., Akesson, T. & Cabane, B. (2010). Ca/Na montmorillonite: structure, forces and swelling properties. *Langmuir* **26**, No. 8, 5782–5790.

Seiphoori, A., Ferrari, A. & Laloui, L. (2014). Water retention behaviour and microstructural evolution of MX-80 bentonite during wetting and drying cycles. *Géotechnique* **64**, No. 9, 721–734.

Sellin, P. & Leupin, O. X. (2013). The use of clay as an engineered barrier in radioactive-waste management – a review. *Clays and Clay Minerals* **61**, No. 6, 477–498.

Sposito, G., Skipper, N. T., Sutton, R., Park, S. H., Soper, A. K. & Greathouse, J. A. (1984). Surface geochemistry of the clay minerals. *Proceedings of the National Academy of Sciences* **96**, No. 7, 3358–3364.

Stern, O. (1924). Zur Theorie der elektrolytischen Doppelschicht (The theory of the electrolytic double-layer). *Zeitschrift für Elektrochemie und Angewandte Physikalische Chemie* **30**, 508–516.

Stçepkowska, E. T. (1990). Aspects of the clay/electrolyte/water system with special reference to the geotechnical properties of clays. *Engineering Geology* **28**, No. 3–4, 249–267.

Sun, W. J., Liu, S. Q., Sun, D. A. & Fang, L. (2014). Swelling characteristics and permeability of bentonite. In *Proceedings of the Sixth International Conference on Unsaturated Soils, UNSAT 2014* (Khalili, N., Russell, A. & Khoshghalb, A., Eds.), Sydney, Australia, pp. 1211–1217.

Swenson, J., Bergman, R. & Howells, W. S. (2000). Quasielastic neutron scattering of two-dimensional water in vermiculite clay. *Journal of Chemical Physics* **113**, No. 7, 2873–2879.

Tessier, D. (1978). Etude de l'organisation des argiles calciques. Evolution au cours de la dessication. *Annales d'Agronomie* **29**, No. 4, 319–355.

Tripathy, S., Sridharan, A. & Schanz, T. (2004). Swelling pressures of compacted bentonites from diffuse double layer theory. *Canadian Geotechnical Journal* **41**, No. 3, 437–450.

Van Olphen, H. (1963). *An introduction to clay colloid chemistry*. John Wiley & Sons.

Van Olphen, H. (1977). *An introduction to clay colloid chemistry: for clay technologists, geologists and soil scientists*. Wiley-Interscience.

Villar, M. V. (2000). *Caracterizacion thermo-hidro-mecanica de una bentonita de Cabo de Gata*. Ph.D. thesis, Universidad Complutense de Madrid.

Villar, M. V. (2002). Thermo-hydro-mechanical characterisation of a bentonite from Cabo de Gata. *Technical report*, CIEMAT.

Villar, M. V. (2007). Water retention of two natural compacted bentonites. *Clays and Clay Minerals* **55**, No. 3, 311–322.

Villar, M. V., Gómez-Espina, R. & Guitiérrez-Nebot, L. (2012). Basal spacings of smectite in compacted bentonite. *Applied Clay Science* **65–66**, 95–105.

Wang, Q. (2012). *Hydro-mechanical behaviour of bentonite-based materials used for high-level radioactive waste disposal*. Ph.D. thesis, Université Paris-Est.

Wang, Q., Cui, Y. J., Tang, A. M., Barnichon, J. D., Saba, S. & Ye, W. M. (2013a). Hydraulic conductivity and microstructure changes of compacted bentonite/sand mixture during hydration. *Engineering Geology* **164**, 67–76.

Wang, Q., Cui, Y. J., Tang, A. M., Li, X. L. & Ye, W. M. (2014). Time- and density-dependent microstructure features of compacted bentonite. *Soils and Foundations* **54**, No. 4, 657–666.

Wang, Q., Tang, A. M., Cui, Y. J., Delage, P., Barnichon, J. D. & Ye, W. M. (2013b). The effects of technological voids on the hydro-mechanical behaviour of compacted bentonite–sand mixture. *Soils and Foundations* **53**, No. 2, 232–245.

Wen, Z. J. (2006). Physical property of China's buffer material for high-level radioactive waste repositories. *Chinese Journal of Rock Mechanics and Engineering* **25**, 794–800.

Wherry, E. T. (1917). Clay derived from volcanic dust in the Pierre of South Dakota. *Washington Academy of Sciences Journal* **7**, 576–583.

Winterkorn, H. F. (1943). The condition of water in porous systems. *Soil Science* **56**, 109–115.

Ye, W. M., Cui, Y. J., Qian, L. X. & Chen, B. (2009). An experimental study of the water transfer through confined compacted GMZ bentonite. *Engineering Geology* **108**, No. 3–4, 169–176.

Yong, R. N., Pusch, R. & Nakano, M. (2009). *Containment of high-level radioactive and hazardous solid wastes with clay barriers*. CRC Press.